Published in final edited form as:
NMR Biomed. 2013 July ; 26(7): 781–787. doi:10.1002/nbm.2870.

Strategies for the development of Gd–based "*q*"–activatable MRI contrast agents

Chuqiao Tu[*] and **Angelique Y. Louie**[*]
Department of Biomedical Engineering, University of California, One Shields Avenue, Davis, CA 95616, USA

Abstract

The emergence and rapid development of activatable contrast agents (CAs), whose relaxivity changes in response to variation of a specific marker in the surrounding physiological microenvironment, have expanded the scope of MRI beyond anatomical and functional imaging to also convey information at the cellular and molecular level. The essence of an activatable MRI CA is the difference in relaxivity before and after a change in a physiological variable - the larger the difference, the better the CA. In this review, strategies for design of activatable Gd CAs, with a switching mechanism based on modulation of hydration (*q*), sensitive to common variables in physiological microenvironment, such as pH, light, redox, and metal ions, are illustrated and discussed.

Keywords

smart contrast agent; reversible switching; gadolinium; spiropyran; luciferase; *in vivo* imaging; redox; NADH

1. Basics of Gd–based activatable MRI CAs

Over the past decade the emergence and rapid development of activatable contrast agents (CAs), whose relaxivity changes report on specific biological activities in the surrounding microenvironment, have enabled MRI to delineate biochemical processes beyond its traditional macroscopic anatomical imaging function (1). The degree of change in relaxivity (Δr) before and after responding to biochemical activity is a key factor in evaluating the efficiency of an activatable CA. To help understand the rationale behind the design of activatable Gd CAs one must look at the major parameters affecting the ability of a Gd CA to alter the relaxation rate (R_1) of water molecules.

The Gd^{3+} ion commonly has a coordination number of 9, meaning it can "bond" to 9 other atoms. Free Gd^{3+} ions are toxic and can substitute for Ca^{2+} ions in the body, thus, Gd CAs used in clinics are typically composed of multidentate ligands such as DOTA (*1,4,7,10*–tetraazacyclododecane–*N,N′,N″,N‴*–tetraacetic acid) or DTPA (diethylene–triamine–pentaacetic acid). These ligands provide 4 oxygen donors and 4 nitrogen donors to sequester the Gd^{3+} ion, preventing the toxic effects of the free ion and leaving one vacancy for water molecules in the inner coordination sphere of Gd(III) (hydration number $q = 1$). Gd CAs can be designed that experience alterations in q in response to biochemical activities such as pH, bioluminescence, redox, and presence of metal ion, etc., resulting in substantial variation in longitudinal relaxivity (r_1) value. The r_1 value of a Gd CA is strongly affected by q, and

[*]Corresponding author, chqtu@ucdavis.edu, aylouie@ucdavis.edu.

higher q typically yields greater relaxivity (2, 3). For example, the r_1 value of Gd–DTPA could increase by approximately 30% if the number of coordinated water molecules increases from 1 to 2 (4). However, safety concerns limit the maximum number of water molecules that should be coordinated to Gd(III) because reduced coordination to the chelate will decrease stability and may result in a release of free Gd^{3+} ions. The range of q values for reported activatable Gd CAs is $2 \geq q \geq 0$, i.e. the denticity of the chelators should not be less than 7 (5).

Two other major factors that influence r_1 values of Gd CAs are water exchange rate and molecular tumbling rate in solution (3). The r_1 value of a Gd CA will be maximal when all protons in the microenvironment of the agent exhibit similar relaxation behavior. This requires a fast exchange rate (k_{ex}) between inner sphere water molecule(s) and bulk water molecules, i.e. an optimal mean residence lifetime of water molecules on Gd(III) (τ_M). However, commercial Gd CAs have typical τ_M values of more than 100 ns, which is far from the optimal τ_M values of approximately 10 ns for these agents. Although τ_M is a very important parameter influencing relaxivity, there are few examples of activatable Gd CAs are designed based on the improvement of this parameter; this is likely due to the relatively small impact on relaxivity that to τ_M has before other parameters are optimized (6, 7). Another mechanism that has been more widely utilized to achieve activation is modulation of tumbling rate. Increased molecular weight can substantially increase the short rotational correlation time (τ_R), i.e. decrease tumbling rate of Gd CAs in biological microenvironment, leading to a substantial increase in r_1 value (3). In this brief review, we will highlight activatable Gd CAs that are designed based on changes in q in response to variables in the biological microenvironment, e.g. luminescence, redox, pH, and metal ions, etc. We focus on more recent reports from the last ten years.

2. Light– and redox–responsive Gd CAs

Bioluminescence is the emission of visible light generated from the chemical energy–to–light conversion from enzyme–catalyzed reactions in living organisms. Bioluminescence has been used for tracking gene expression, studying cell fate and function, and understanding protein–protein interaction, etc. Therefore, imaging bioluminescence can provide valuable means for monitoring different biological processes in immunology, oncology, virology, and neuroscience (8). While optical imaging of bioluminescence offers the benefit of convenience and high sensitivity, it has the drawback of limited tissue penetration depth. In contrast, a Gd CA whose relaxivity can be tuned by light would allow MRI to be responsive to bioluminescence in deep tissues. In this section we discuss our work towards developing light–sensitive agents.

2.1 Design of light–responsive Gd CAs

Spiro(benzo)pyrans (SP) and spiro(naphth)oxazines (SO) are among the most widely studied classes of photochromic compounds. The spiropyran or spirooxazine molecule is stable in its closed–ring (SP and SO) isomeric form as a colorless or pale yellow solution, while UV irradiation can break the C–O bond between the sp^3-hybridized "spiro" carbon (marked in red in Fig. 1) and the pyran/oxazine part, producing a metastable open–ring isomer (MC), which has an optical absorption peak at 550–600 nm (9, 10). The original colorless form of SP or SO can be restored either *via* visible light irradiation or thermal relaxation. There have been a number of reports on metal ion bound crown ether conjugates conjugated to a spiropyran molecule. In these structures the MC isomer is known to participate in coordination of the bound metal ion through a phenolate anion, while the SP isomer does not, and light irradiation triggers immediate isomerization between the two isomers (11–13). By substituting the crown ether moiety with a macrocyclic ligand DO3A (*1,4,7,10*–tetraazacyclododecane–*1,4,7*–trisacetic acid) known to bind Gd^{3+} ion, we hypothesized that

upon UV/vis light irradiation, the MC–SP structural change of the attached spiropyran moiety would modify the number of coordinating ligands to Gd, thus altering hydration number *q*. We have developed a number of variants for these types of light–responsive Gd agents in an effort to use structure to modify function (14–16).

2.2 The first generation light–responsive Gd CA

The first generation agent was based on the conjugation of a spirobenzopyran moiety to a Gd–DO3A chelate (Fig. 1) (14). We hypothesized that in the MC form there should be only one water molecule in the first coordination sphere of Gd(III) due to the presence of the phenoxide anion, and its r_1 value should be similar to that of Gd–DOTA (~ 4 $mM^{-1}•s^{-1}$) (17). Visible light irradiation would trigger isomerization of the MC isomer to the SP isomer. The number of water molecules in the first coordination sphere of Gd(III) should increase to two and the r_1 value of the SP isomer should have a substantial increase (17, 18), similar to the situation in Fig. 2. The synthesized spirobenzopyran–Gd–DO3A complex was yellow colored (at higher concentrations this was orange) in the aqueous solution and had a distinct absorption at 468 nm. UV irradiation at 365 nm could not further increase the absorption, indicating the agent was in its MC form. Irradiation with visible light for 1 min greatly diminished the absorption at 468 nm and the color of the solution quickly faded to pale yellow, representing a mixture of MC and SP isomers. UV irradiation at 365 nm could only partially restore the absorption at 468 nm. However, the absorption could be completely restored after the sample was put in dark for 20 minutes.

The effect of limited isomerization of spirobenzopyran–Gd–DO3A on the r_1 relaxivity was evaluated at 1.4 T and 37 °C. The complex stored in dark, i.e. MC isomer, had an r_1 value of 3.72 $mM^{-1}•s^{-1}$, and the isomer obtained via visible light irradiation, i.e. the mixture of MC and SP, had an r_1 value of 2.93 $mM^{-1}•s^{-1}$. Thus, spirobenzopyran–Gd–DO3A showed a 21% decrease in r_1 relaxivity upon visible light irradiation (14). The result deviated from our expectation that SP isomer of spirobenzopyran–Gd–DO3A would have a higher r_1 value because this isomer would have two coordination vacancies left for water molecules. This unexpected result may be explained by the structural distinction between MC and SP isomeric forms. In SP form, the indoline part is orthogonal to the benzopyran part. Therefore, the Gd(III) may have electrostatic interaction with lone pairs of electrons in oxygen and nitrogen atoms of the spirobenzopyran indoline part, as shown in Fig.1. In addition, the “indoline cap” may sterically hinder the water molecules from accessing the Gd(III), and inhibits MRI contrast enhancement. In MC isomeric form, the break of C–O bond removes the “indoline cap”, allowing the water molecules to access the Gd(III) center more readily.

2.3 The second generation light–responsive Gd CA, a redox–response plus

Considering that the small relaxivity difference of the first generation agent may be due to the incomplete conversion from MC to SP isomer upon light irradiation, a strong electron–withdrawing nitro group was attached to the indole ring of the spirobenzopyran (15). The nitro group can destabilize formation of the positive charge carried in the iminium form of the MC isomer (Fig. 1), thus shifting the equilibrium of the complex back towards the SP isomer, which may lead to an enlarged gap in relaxivity between the two isomers. The photochromic behavior of dinitrospirobenzopyran–Gd–DO3A is similar to that of the first generation agent, but with a longer absorption wavelength centered at 502 nm and the irradiation with visible light resulted in an almost complete loss of the absorbance peak. However, the dinitrospirobenzopyran–Gd–DO3A only presented an 18% decrease in r_1 relaxivity upon light stimulus (from 2.51 (MC) to 2.05 (SP) $mM^{-1}•s^{-1}$). Interestingly, the dinitrospirobenzopyran–Gd–DO3A was found to be responsive to reduced nicotinamide adenine dinucleotide (NADH), the principal electron donor for the respiratory chain in

mammalian cells, a property that was not observed for the first generation agent. After mixing with NADH, dinitrospirobenzopyran–Gd–DO3A exhibited a steady decrease in absorbance at 502 nm. The absorbance decrease rate corresponded to the concentration of NADH employed, and the r_1 value was shown to decrease by up to 26%, to 1.86 $mM^{-1}•s^{-1}$. Aqueous solutions in dark with a series of Gd concentrations of dinitrospirobenzopyran–Gd–DO3A were imaged at 7T. After irradiation with visible light or mixing with NADH, the solutions were imaged again under the same conditions. The signal intensity in MRI of dinitrospirobenzopyran–Gd–DO3A did not have observable change after visible light irradiation. However, the intensity did decrease after mixing with NADH.

2.4 The third generation light–responsive Gd CA, a strong redox–response

A further modification was to utilize spironaphthoxazine as the light sensitive moiety, which has a similar isomerization mechanism to spiropyran compounds (16). However, the photochromic behavior of spironaphthoxazine–Gd–DO3A differed substantially from the spiropyran–based agents. Spironaphthoxazine–Gd–DO3A in water had a distinct absorption at 440 nm in the dark. Irradiation with UV at 365 nm slightly increased the absorption at 440 nm. After visible light irradiation, the solution still had an obvious absorption at 440 nm, indicating that visible light irradiation only partially converted the MC isomer to the closed SO form. After irradiation with visible light, subsequent recovery of the absorbance at 440 nm, either by irradiation with UV at 365 nm or storage in the dark, was limited. The relaxivity change upon light stimulation was small (< 10%), probably due to the limited isomerization of the spironaphthoxazine–Gd–DO3A, but was in the direction theoretically predicted and relaxivity was higher for the SO form, unlike the spiropyran compounds. The optical and magnetic properties of spironaphthoxazine–Gd–DO3A and (dinitro)spirobenzopyran–Gd–DO3A are summarized in Table 1.

Although spironaphthoxazine–Gd–DO3A did not respond well to light, it had a very strong response to NADH, verified by the rapid and significant decrease of absorption at 440 nm; the increase in absorption at 259 nm representing NAD^+, the oxidized product of NADH; and the decrease of absorption at 339 nm for NADH. After the initial rapid decrease, the absorption peak at 440 nm continued to decrease slowly. Similar to the reaction of dinitrospirobenzopyran–Gd–DO3A and NADH, the observed reaction rate of spironaphthoxazine–Gd–DO3A and NADH was dependent upon the mole ratio of NADH to gadolinium. The absorption profile of NADH did not change when mixing NADH with Gd–DOTA or aqueous $GdCl_3$ solution, indicating that the response of spironaphthoxazine–Gd–DO3A to NADH occurred in its spironaphthoxazine part.

After the reaction of spironaphthoxazine–Gd–DO3A and NADH, hydrogen peroxide (3:1, H_2O_2:NADH) was applied to the system. The absorption at 440 nm was quickly and partially (~ 1/3) restored, then the change in absorption was slow, indicating the incomplete reversal to MC isomer from the reduced product of spironaphthoxazine–Gd–DO3A. The reaction with NADH substantially influenced the hydration state of Gd(III) center and changed the r_1 value of spironaphthoxazine–Gd–DO3A. In the dark the Gd(III) agent had an r_1 value of 5.58 $mM^{-1}•s^{-1}$ and an average of 1.26 water molecules in the inner coordination sphere of Gd(III). When NADH was added, the hydration number (q) increased to 2.01, leading to an r_1 value increase of 54%. After reaction with NADH, the T_1 value of spironaphthoxazine–Gd–DO3A could be fully restored when addition of hydrogen peroxide to the system, indicating the redox response of the agent was reversible. Macrophages incubated with spironaphthoxazine–Gd–DO3A and exposed to extracellularly applied NADH showed substantial MRI contrast enhancement, as shown in Fig. 2.

The mechanism of relaxivity change of spironaphthoxazine–Gd–DO3A upon mixing with NADH fits with our original hypothesis for the mechanism of activation when we designed

these light–responsive Gd CAs, as shown in Fig. 2. In MC isomer Gd(III) was coordinated by a phenolate anion and seven other atoms. It had a hydration number q of 1.26. When NADH induced the isomerization of spironaphthoxazine–Gd–DO3A to the SO form, the C–O was restored which resulted in removal of the phenoxide oxygen anion from the inner coordination sphere of Gd(III). An additional water molecule could access the gadolinium ion and the hydration number q increased to 2.

2.5 Determination of hydration number *q*

Various methods have been reported for the determination of q in Gd(III) chelates including X–ray crystallography, luminescence lifetime spectroscopy of Eu(III) or Tb(III) analogs, and variable temperature ^{17}O NMR linewidth measurements (3). X–Ray crystallography can accurately reveal the coordination sphere of Gd(III) center in solid state but may not be able to provide useful information when the complexes are in aqueous solutions or bound to a protein. Luminescence spectroscopy can indirectly estimate the hydration number of Gd(III) center by measuring fluorescence quench of Eu(III) or Tb(III) analog in water and deuterium oxide. In general, ^{17}O NMR experiments require a surrogate complex as well as the Gd(III) complex, in most cases a Dy(III) or Tb(III) complex, because it does not have a large line broadening which is necessary for an accurate determination of the shift. However, the exchange between Gd(III) bound water and bulk water is fast on the ^{17}O NMR time scale at the temperatures of about 80 °C, enabling Gd(III) complexes to be directly used in ^{17}O NMR experiments, because the fast water exchange can effectively decrease the line width of Gd(III) complexes (19). In practice, we found that the line width of Gd(III) complexes are not worse than reported Dy(III) complexes at elevated temperatures (16). Therefore, the ^{17}O NMR spectroscopy is a convenient and efficient method for hydration number (q) measurement of Gd(III) centers that uses Gd(III) complexes themselves rather than surrogate complexes.

3. pH–responsive Gd CAs

A great interest in developing pH–responsive Gd CAs arose from the discovery that the extracellular medium in tumor tissues and various ischemic tissues is slightly acidic compared to normal tissues. Therefore, pH variation could be a marker for early detection and treatment of tumors and ischemic diseases (20). The common design approach for generating pH–responsive Gd CAs is to modify the ligand's denticity upon a protonation/deprotonation step.

Gd chelates exhibiting pH–dependent r_1 relaxivity by virtue of a switch in hydration state were reported by Aime and coworkers. The pH values of these agents were controlled by the on/off ligation of a sulfonamide nitrogen donor. One carboxymethyl group of Gd–DOTA was replaced by proton–ionizable α–arylsulfonamide groups with pK_a values of 5.7, 6.4, and 6.7 for the CF_3, CH_3, and OCH_3 substituents, respectively (21). The r_1 values of these Gd agents were recorded as a function of pH in the range 4–10 (Fig. 3). At pH 5, the limiting r_1 value was 7.8 $mM^{-1}•s^{-1}$ and fell to 2.6 $mM^{-1}•s^{-1}$ at pH 8 for the OCH_3 derivative (300 MHz, 25 °C). Measurements of the pH dependence of the isomers revealed that the hydration number $q = 0$ at pH 8 and $q = 2$ at pH 5 (21, 22).

4. Metal ion–responsive MRI CAs

MRI CAs sensitive to transition metal ions such as calcium, zinc, iron, and copper ions have been of great interest because these biologically relevant metal ions play significant roles in the biochemical processes that control biological signaling, redox homeostasis, and metabolism, etc. (23, 24). A common strategy for design of metal ion–responsive Gd CAs is illustrated in Fig. 4. The Gd CA consists of two different subunits: one acts as Gd^{3+} ion

chelator and the other has high selectivity towards the target metal ion. In the absence of metal ions, one or two donor atoms from the target metal ion coordination subunit (highlighted in red in Fig. 4), plus one or zero water molecules depending on the coordination status of Gd(III), complete the inner coordination sphere of Gd(III). In the presence of the target metal ions, the donor atoms leave the Gd(III) center and coordinate to the target metal ion together with other donor atoms of the subunit, liberating space for one or two water molecules to occupy the vacated site at the inner coordination sphere of Gd(III). The r_1 value increases in correspondence to the increase of hydration number *q*.

Monitoring intracellular calcium levels is of intense interest, due in particular to its critical role in cell signaling. Meade and coworkers synthesized Ca^{2+} ion responsive MRI CAs by connecting two Gd–DO3A chelates with a modified BAPTA (1,2–bis(*o*–aminophenoxyl)–ethane–*N,N,N′,N′*–tetraacetic acid) linker that carried two aromatic iminodiacetate groups (25). In the presence of Ca^{2+} ion, the two iminoacetate groups, originally coordinated to the two Gd(III), rearranged and bound one Ca^{2+} ion. Two water molecules filled the resulting vacant coordination sites on the two Gd(III) centers, leading to a substantial r_1 value increase from 3.26 to 5.76 $mM^{-1}•s^{-1}$. The change in relaxivity was most striking in the Ca^{2+} ion concentration range of 0.1 to 10 μM which is close to the concentration of Ca^{2+} ion within cells (0.02–0.1 μM), making this Gd CA promising for detecting intracellular calcium related activities such as signal transduction and regulation, muscle contraction, and blood–clotting cascade, etc. Later, Gd CAs with varying linkers were developed (26–31). Their relaxivity responds to Ca^{2+} ion concentration ranging from millimolar to micromolar, making them promising as extracellular calcium sensors as well.

The development of Cu–sensing Gd CAs is relatively new in comparison with other biological metal ions. Chang and coworkers developed a series of Gd–based Cu sensors that utilized a Gd–DO3A core with a Cu ion binding pendant arm (32–34). These agents modulated r_1 values through altering hydration state of the Gd(III). Upon addition of Cu^{+} or Cu^{2+} ion, the r_1 values of these agents could increase up to 4.6–fold. The similar strategy has been used to develop more Cu^{2+}–responsive Gd CAs (35, 36). Gd–QDOTAMA (QDOTAMA: *1*– (*N*–quinolin–*8*–yl–acetamide) –*4,7,10*–*tris*(acetic acid) –*1,4,7,10*–tetraazacyclododecane) contained a Gd–DO3A core and a quinoline–based pendant arm (35). The agent's r_1 value increased from 4.27 $mM^{-1}•s^{-1}$ to 7.29 $mM^{-1}•s^{-1}$ in response to equimolar amounts of Cu^{2+} ion. There were no distinct changes in relaxivity upon addition of alkali metal cations (K^{+} or Na^{+}), alkaline earth metal cations (Mg^{2+} or Ca^{2+}), or *d*–block metal cations (Zn^{2+}, Cu^{+}, Fe^{2+}, Fe^{3+}), indicating that Gd–QDOTAMA was highly selective for Cu^{2+} ion over other biologically relevant metal ions.

5. Perspective: overcoming major challenges to clinical application of activatable CAs

Besides delivery to the tissue of interest, one of the most critical and widely discussed challenges for the use of activatable agents *in vivo* is how to assure that the measurement of the MR contrast reports on the physiological variable of interest only, not on a change in the local concentration of the activatable agent (6, 37, 38). This is particularly true for biochemical processes that will not change during the course of examination, so that there is no clear “off/on” response. Where the microenvironment conditions are static, the intensity of signal (i.e. T_1) alone must somehow be correlated with the state of activation of the agent and not dependent on concentration of the agent. To be able to do this, there must be a reliable method to determine contrast agent concentration so that its contribution can be deconvolved from the data.

Multimodal imaging methods have the potential to allow quantification of local CA concentrations and thus decouple CA concentration from observed contrast (39). This principle has recently been demonstrated using dual MRI/PET(SPECT) (positron emission tomography/single photon emission computed tomography) probes. A dual MRI/PET probe was reported by Caravan and coworkers who covalently conjugated a ^{18}F containing moiety to a Gd chelate whose relaxivity is pH dependent (40). It was found that the PET moiety could report the local concentration of the paramagnetic agent, which thus accounted for contributions to the observed signal arising from changes in the amount of Gd agent present. Another dual system, MRI/SPECT, was reported by Aime and coworkers, which is based on the pH–sensitive Gd chelate described earlier in section 3. The system contains two chelates that differ only in the coordinated lanthanide(III) ion being Gd(III) for MRI and Ho(III) for SPECT, in the expectation that Ho(III)–L and Gd(III)–L should experience similar biodistribution when administered *in vivo*. (Fig. 5A) (22). A phantom consisting of four tubes corresponding to the concentrations of lanthanide(III) complexes and pH was subjected to neutron irradiation which transformed ^{165}Ho (SPECT inactive) into ^{166}Ho that emits γ–radiation ($t_{½}$ = 26.6 h). The samples underwent γ–counting and the Ho(III) concentrations of the four samples were extracted by the use of previously determined calibration lines, and from these the corresponding Gd(III) concentrations were calculated. MR imaging of the four samples were performed on a Bruker 300 spectrometer. MR signal intensities were normalized to the relative Gd(III)–concentrations calculated on the basis of the γ–counter measurements. As shown in the Fig. 5B, the signal progressively decreased from sample 1 to sample 4 as expected from the pH dependence of the relaxivity of the Gd–L system. The authors obtained a linear correspondence between the pH, measured by a pH electrode, and the values determined by the SPECT/MRI probe through the use of the relationship between the relaxivity and pH (Fig. 3 & Fig. 5B).

Concluding Remarks

During the last decade a number of Gd CAs responsive to diagnostically relevant biochemical markers have been reported. With r_1 values varying up to several folds in *in vitro* experiments, these CAs have great potential to monitor metabolic reactions and detect diseases at the cellular and molecular levels. However, to date only very few examples have been tested *in vivo*, indicating more work has to be done in this field and there are critical issues that need to be addressed before the full potential of this exciting approach to molecular imaging can be realized. Sensitivity is also a frequent challenge due to low tissue concentrations of many biochemical markers of interest (nanomolar scale) and the necessity of relatively high levels of MRI CAs (millimolar scale) (41). The field of activatable CAs has shown wonderful potential in the laboratory but is still in its infancy for clinical translation. An effective collaboration between chemists, biologists, and clinicians will be crucial in bringing activatable CAs with outstanding physical properties into realistic uses.

Acknowledgments

The authors wish to acknowledge the NIH–NIBIB (R01 EB000993) for support of this work.

ABBREVIATIONS

BAPTA	*1,2*–bis(*o*–aminophenoxyl)–ethane–*N,N,N′,N′*–tetraacetic acid
CAs	contrast agents
DOTA	*1,4,7,10*–tetraazacyclododecane–*N,N′,N″,N‴*–tetraacetic acid
DO3A	*1,4,7,10*–tetraazacyclododecane–*1,4,7*–trisacetic acid

DTPA	diethylene–triamine–pentaacetic acid
k_{ex}	water exchange rate
MC	metastable open–ring isomer of spiro(naphth)oxazines or spiro(benzo)pyrans
NAD	nicotinamide adenine dinucleotide
NADH	reduced nicotinamide adenine dinucleotide
PET	positron emission tomography
q	hydration number
QDOTAMA	*1*– (*N*–quinolin–*8*–yl–acetamide) –*4,7,10*–*tris*(acetic acid) –*1,4,7,10*–tetraazacyclododecane
r_1	longitudinal relaxivity
R_1	longitudinal relaxation rate
SO	closed ring isomer of spiro(naphth)oxazines
SP	closed ring isomer of spiro(benzo)pyrans
SPECT	single photon emission computed tomography
τ_R	rotational correlation time
τ_M	mean residence lifetime of water molecules

REFERENCES

1. Tu CQ, Osborne EA, Louie AY. Activatable T (1) and T (2) Magnetic Resonance Imaging Contrast Agents. Ann. Biomed. Eng. 2011; 39(4):1335–1348. [PubMed: 21331662]
2. Toth E, Helm L, Merbach AE. Relaxivity of MRI contrast agents. Contrast Agents I. 2002; 221:61–101.
3. Caravan P. Strategies for increasing the sensitivity of gadolinium based MRI contrast agents. Chem. Soc. Rev. 2006; 35(6):512–523. [PubMed: 16729145]
4. Burtea, C.; Laurent, S.; Elst, LV.; Muller, RN. Contrast Agents: Magnetic Resonance. In: Semmler, W.; Schwaiger, M., editors. Molecular Imaging I: Handbook of Experimental Pharmacology. Heidelberg: Springer-Verlag Berlin; 2008. p. 135-165.
5. Querol, M.; Bogdanov, A. Environment-sensitive and Enzyme-sensitive MR Contrast Agents. In: Semmler, W.; Schwaiger, M., editors. Molecular Imaging II. Handbook of Experimental Pharmacology. Berlin: Springer-Verlag; 2008. p. 37-57.
6. Garcia-Martin ML, Martinez GV, Raghunand N, Sherry AD, Zhang SR, Gillies RJ. High resolution pH(e) imaging of rat glioma using pH-dependent relaxivity. Magn. Reson. Med. 2006; 55(2):309–315. [PubMed: 16402385]
7. Zhang SR, Wu KC, Sherry AD. A novel pH-sensitive MRI contrast agent. Angew. Chem. Int. Edit. 1999; 38(21):3192–3194.
8. Badr CE, Tannous BA. Bioluminescence imaging: progress and applications. Trends Biotechnol. 2011; 29(12):624–633. [PubMed: 21788092]
9. Zhi JF, Baba R, Hashimoto K, Fujishima A. Photoelectrochromic properties of a spirobenzopyran derivative. J. Photochem. Photobiol. A-Chem. 1995; 92(1–2):91–97.
10. Berkovic G, Krongauz V, Weiss V. Spiropyrans and spirooxazines for memories and switches. Chem. Rev. 2000; 100(5):1741–1753. [PubMed: 11777418]
11. Wojtyk JTC, Kazmaier PM, Buncel E. Effects of metal ion complexation on the spiropyranmerocyanine interconversion: development of a thermally stable photo-switch. Chem. Commun. 1998; (16):1703–1704.

12. Chibisov AK, Gorner H. Complexes of spiropyran-derived merocyanines with metal ions: relaxation kinetics, photochemistry and solvent effects. Chem. Phys. 1998; 237(3):425–442.
13. Gorner H, Chibisov AK. Complexes of spiropyran-derived merocyanines with metal ions - Thermally activated and light-induced processes. J. Chem. Soc.-Faraday Trans. 1998; 94(17): 2557–2564.
14. Tu CQ, Louie AY. Photochromically-controlled, reversibly-activated MRI and optical contrast agent. Chem. Commun. 2007; (13):1331–1333.
15. Tu CQ, Osborne EA, Louie AY. Synthesis and characterization of a redox- and lightsensitive MRI contrast agent. Tetrahedron. 2009; 65(7):1241–1246. [PubMed: 20126289]
16. Tu C, Nagao R, Louie AY. Multimodal Magnetic-Resonance/Optical-Imaging Contrast Agent Sensitive to NADH. Angew. Chem. Int. Edit. 2009; 48(35):6547–6551.
17. Caravan P, Ellison JJ, McMurry TJ, Lauffer RB. Gadolinium(III) chelates as MRI contrast agents: Structure, dynamics, and applications. Chem. Rev. 1999; 99(9):2293–2352. [PubMed: 11749483]
18. Aime S, Botta M, Bruce JI, Mainero V, Parker D, Terreno E. Modulation of the water exchange rates in Gd-DO3A complex by formation of ternary complexes with carboxylate ligands. Chem. Commun. 2001; (01):115–116.
19. Djanashvili K, Peters JA. How to determine the number of inner-sphere water molecules in lanthanide(III) complexes by O-17 NMR spectroscopy. A technical note. Contrast Media Mol. Imaging. 2007; 2(2):67–71. [PubMed: 17451189]
20. Perez-Mayoral E, Negri V, Soler-Padros J, Cerdan S, Ballesteros P. Chemistry of paramagnetic and diamagnetic contrast agents for Magnetic Resonance Imaging and Spectroscopy pH responsive contrast agents. Eur. J. Radiol. 2008; 67(3):453–458. [PubMed: 18455343]
21. Lowe MP, Parker D, Reany O, Aime S, Botta M, Castellano G, Gianolio E, Pagliarin R. pH-dependent modulation of relaxivity and luminescence in macrocyclic gadolinium and europium complexes based on reversible intramolecular sulfonamide ligation. J. Am. Chem. Soc. 2001; 123(31):7601–7609. [PubMed: 11480981]
22. Gianolio E, Maciocco L, Imperio D, Giovenzana GB, Simonelli F, Abbas K, Bisi G, Aime S. Dual MRI-SPECT agent for pH-mapping. Chem. Commun. 2011; 47(5):1539–1541.
23. Bonnet CS, Toth E. MRI probes for sensing biologically relevant metal ions. Future Med. Chem. 2010; 2(3):367–384. [PubMed: 21426172]
24. Que EL, Chang CJ. Responsive magnetic resonance imaging contrast agents as chemical sensors for metals in biology and medicine. Chem. Soc. Rev. 2010; 39(1):51–60. [PubMed: 20023836]
25. Li, W-h; Fraser, SE.; Meade, TJ. A Calcium-Sensitive Magnetic Resonance Imaging Contrast Agent. J. Am. Chem. Soc. 1999; 121(6):1413–1414.
26. Dhingra K, Fousková P, Angelovski G, Maier M, Logothetis N, Tóth É. Towards extracellular Ca2+ sensing by MRI: synthesis and calcium-dependent 1H and 17O relaxation studies of two novel bismacrocyclic Gd3+ complexes. J. Biol. Inorg. Chem. 2008; 13(1):35–46. [PubMed: 17874148]
27. Mishra A, Fousková P, Angelovski G, Balogh E, Mishra AK, Logothetis NK, Tóth É. Facile Synthesis and Relaxation Properties of Novel Bispolyazamacrocyclic Gd3+ Complexes: An Attempt towards Calcium-Sensitive MRI Contrast Agents. Inorg. Chem. 2008; 47(4):1370–1381. [PubMed: 18166011]
28. Angelovski G, Fouskova P, Mamedov I, Canals S, Toth E, Logothetis NK. Smart Magnetic Resonance Imaging Agents that Sense Extracellular Calcium Fluctuations. ChemBioChem. 2008; 9(11):1729–1734. [PubMed: 18604834]
29. Mishra A, Logothetis NK, Parker D. Critical In Vitro Evaluation of Responsive MRI Contrast Agents for Calcium and Zinc. Chem.-Eur. J. 2011; 17(5):1529–1537. [PubMed: 21268155]
30. Kubíček V, Vitha T, Kotek J, Hermann P, Vander Elst L, Muller RN, Lukeš I, Peters JA. Towards MRI contrast agents responsive to Ca(II) and Mg(II) ions: metal-induced oligomerization of dota-bisphosphonate conjugates. Contrast Media Mol. Imaging. 2010; 5(5):294–296. [PubMed: 20973114]
31. Mamedov I, Logothetis NK, Angelovski G. Structure-related variable responses of calcium sensitive MRI probes. Org. Biomol. Chem. 2011; 9(16):5816–5824. [PubMed: 21727986]

32. Que EL, Chang CJ. A smart magnetic resonance contrast agent for selective copper sensing. J. Am. Chem. Soc. 2006; 128(50):15942–15943. [PubMed: 17165700]

33. Que EL, Gianolio E, Baker SL, Wong AP, Aime S, Chang CJ. Copper-Responsive Magnetic Resonance Imaging Contrast Agents. J. Am. Chem. Soc. 2009; 131(24):8527–8536. [PubMed: 19489557]

34. Que EL, Gianolio E, Baker SL, Aime S, Chang CJ. A copper-activated magnetic resonance imaging contrast agent with improved turn-on relaxivity response and anion compatibility. Dalton Trans. 2010; 39(2):469–476. [PubMed: 20023983]

35. Li WS, Luo JA, Chen ZN. A gadolinium(III) complex with 8-amidequinoline based ligand as coppeRII) ion responsive contrast agent. Dalton Trans. 2011; 40(2):484–488. [PubMed: 21113542]

36. Kasala D, Lin TS, Chen CY, Liu GC, Kao CL, Cheng TL, Wang YM. Gd(Try-TTDA)(H(2)O)(2-): A new MRI contrast agent for copper ion sensing. Dalton Trans. 2011; 40(18):5018–5025. [PubMed: 21451883]

37. Aime S, Fedeli F, Sanino A, Terreno E. A R2/R1 Ratiometric Procedure for a Concentration-Independent, pH-Responsive, Gd(III)-Based MRI Agent. J. Am. Chem. Soc. 2006; 128(35):11326–11327. [PubMed: 16939235]

38. Morawski AM, Winter PM, Yu X, Fuhrhop RW, Scott MJ, Hockett F, Robertson JD, Gaffney PJ, Lanza GM, Wickline SA. Quantitative "magnetic resonance immunohistochemistry" with ligand-targeted F-19 nanoparticles. Magn. Reson. Med. 2004; 52(6):1255–1262. [PubMed: 15562481]

39. Louie A. Multimodality Imaging Probes: Design and Challenges. Chem. Rev. 2010; 110(5):3146–3195. [PubMed: 20225900]

40. Frullano L, Catana C, Benner T, Sherry AD, Caravan P. Bimodal MR-PET Agent for Quantitative pH Imaging. Angew. Chem. Int. Edit. 2010; 49(13):2382–2384.

41. Tu CQ, Louie AY. Nanoformulations for molecular MRI. WIREs Nanomed. Nanobiotechnol. 2012

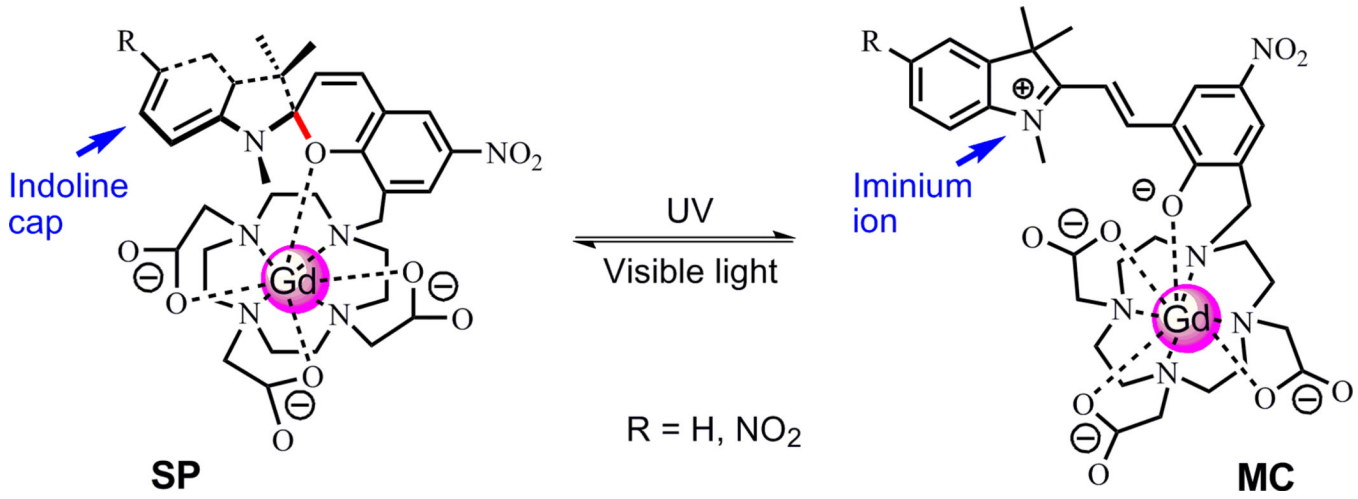

Figure 1.
Proposed isomerization of (dinitro)spirobenzopyran–Gd–DO3A under UV/vis light stimulation. Images modified from Ref (14, 15).

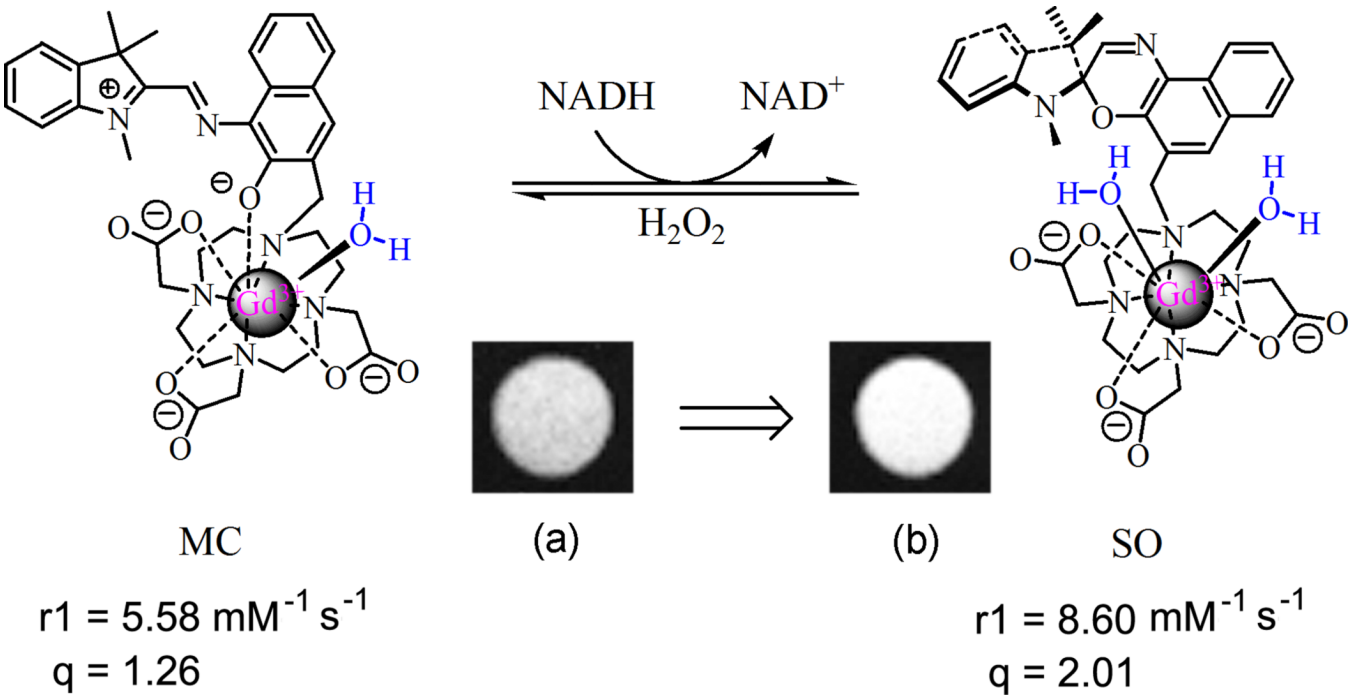

Figure 2.
The structural, r_1 relaxivity, and hydration number (q) changes of spironaphthoxazine–Gd–DO3A triggered by NADH and hydrogen peroxide. Image from Ref (1) which was modified from Ref (16).

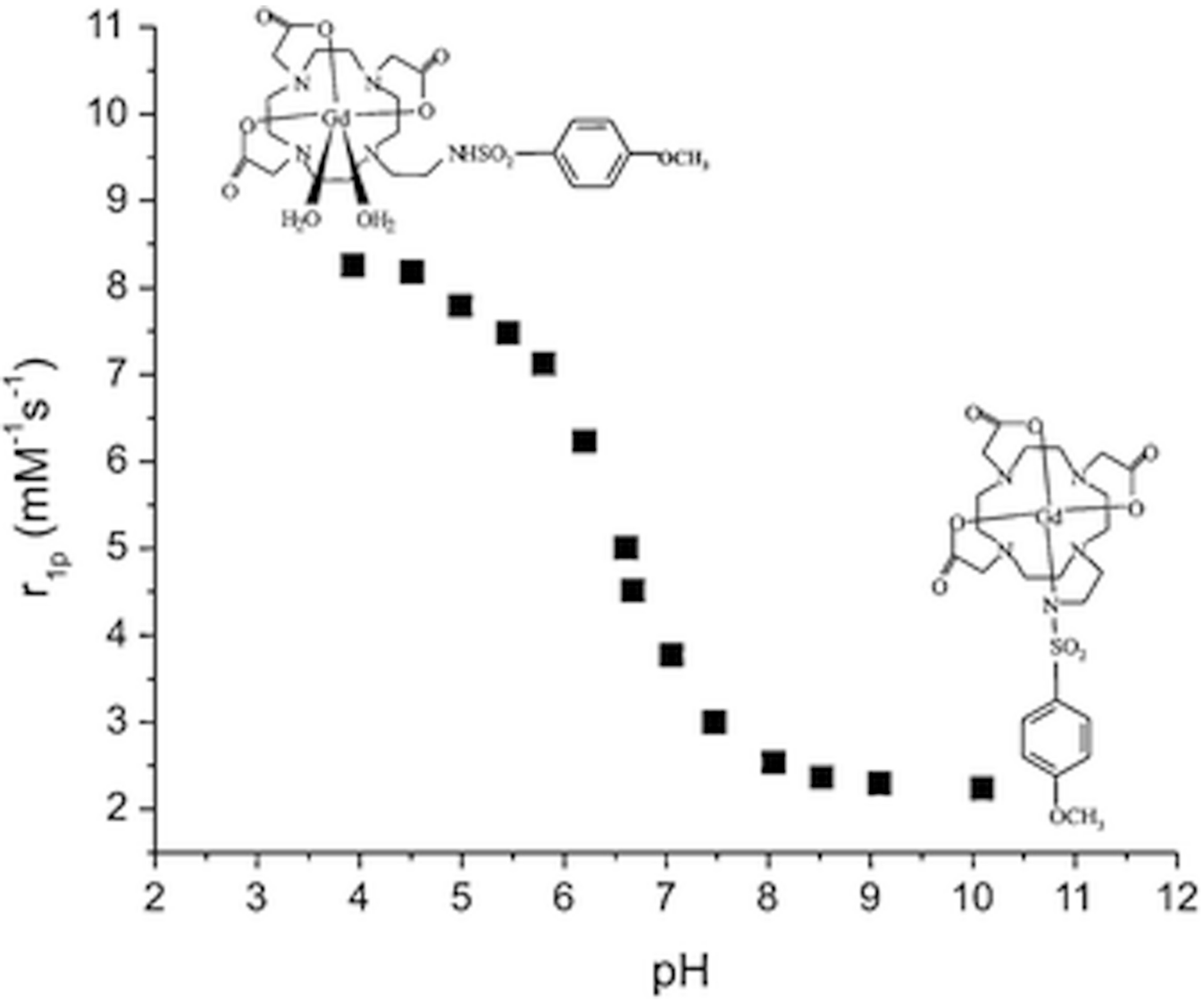

Figure 3.
Relaxivity (r_1)–pH dependence of 1-[2'-(4-Methoxyphenylsulfonyl-amino)ethyl]–Gd–DOTA measured at 300 MHz and 25 °C. Image from Ref (22).

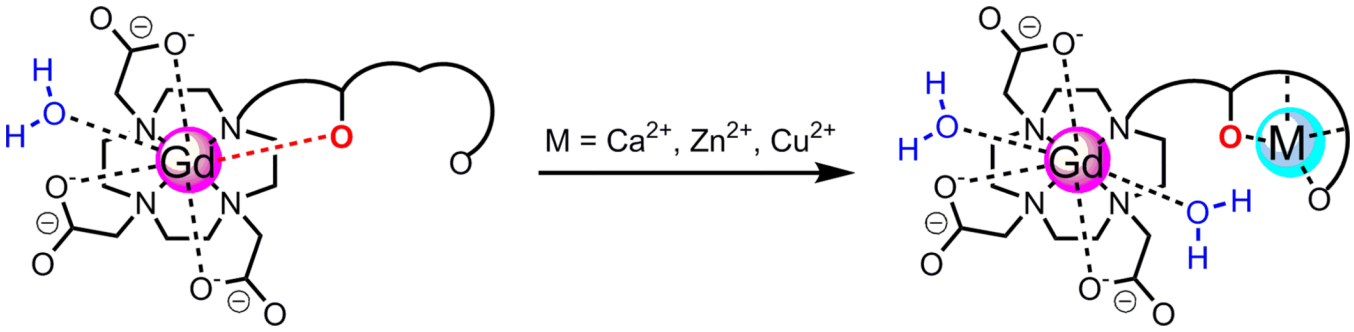

Figure 4.
Schematic illustration of metal ion–responsive Gd CAs.

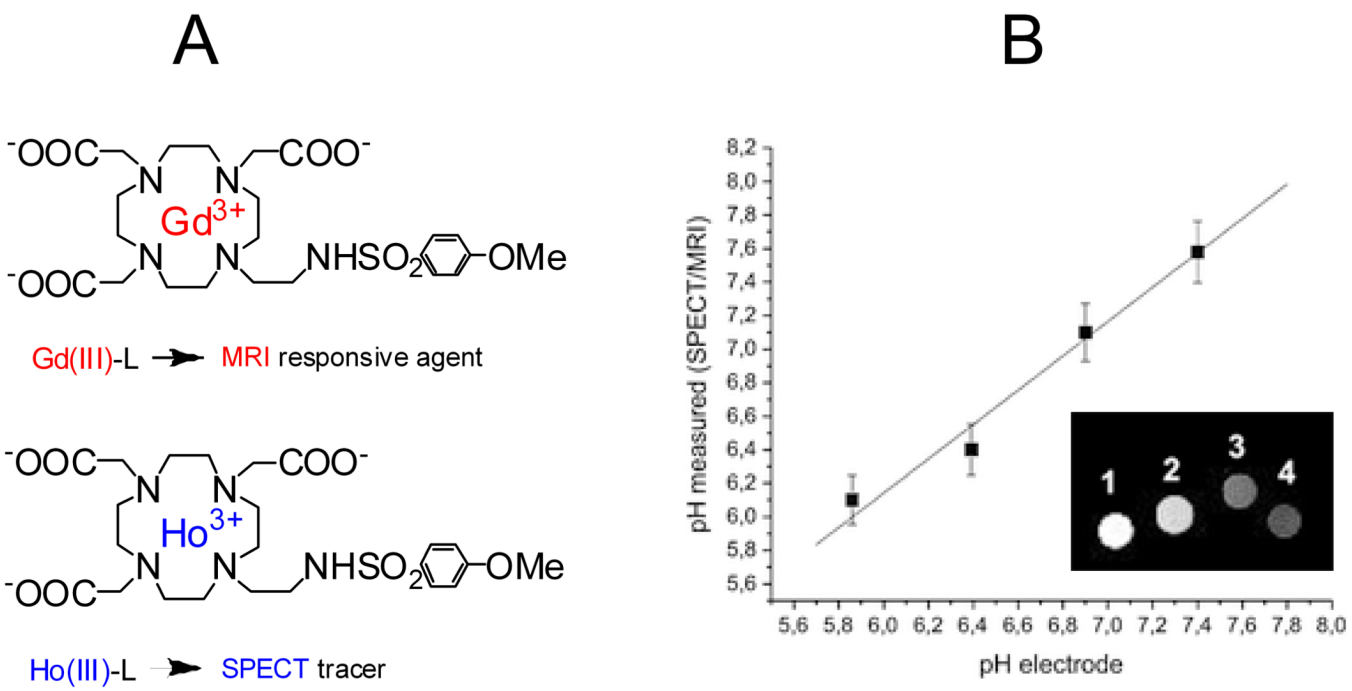

Figure 5.

A: The dual MRI/SPECT system that contains two lanthanide(III) ion chelates. B. Relationship between the pH values measured through pH–electrode and through SPECT/MRI analysis. Inset: MRI images of the phantom containing the four samples at (1) pH 5.9; (2) pH 6.4; (3) pH 6.9; (4) pH 7.4 after normalization with respect to the Gd(III) concentration of the four samples determined via SPECT measurements. Images from Ref (22).

Table 1

The summary of optical properties, photoisomerization, and r_1 relaxivity change of spiropyran– and spirooxazine–based activatable Gd CAs.

Light-responsive Gd CAs	Absorption	Absorbance value			Reversibility	r_1 relaxivity ($mM^{-1}•s^{-1}$)		
		Dark	Light	Change		Dark	Light	Change
Spiropyran–Gd–DO3A	468 nm	1.09	0.37	66%	Yes	3.72	2.93	21%
Dinitrospiropyran–Gd–DO3A	502 nm	0.69	0.14	80%	Yes	2.51	2.05	14%
Spirooxazine–Gd–DO3A	440 nm	0.84	0.64	24%	No	5.58	5.93	6%